

A Detailed Assessment of the Korumburra Earthquake Cluster, 2009

Bathgate, J.¹, Allen, T.², Clark, D.², Collins, C.², Gibson G.³, Glanville, H.¹, Pascale, A.⁴, Peck, W.⁴, Quinn, C.⁴, & Tatham, S.¹

Introduction

A series of earthquakes with epicentres near Korumburra in southeast Victoria commenced in January 2009 and has continued through to November 2009. On March 6 an earthquake of magnitude ML 4.6 occurred which was felt over a wide area of Victoria, including Melbourne. Following this earthquake six temporary seismographs were deployed near the epicentre by Environmental Systems and Services (ES&S), Gary Gibson, and Geoscience Australia (GA). These recorders complemented the permanent networks operated by GA and ES&S, capturing many aftershocks and a second magnitude 4.6 earthquake on March 18. Preliminary hypocentres were determined from the permanent station data, and were refined using additional data from the temporary stations. A depth of about 6 km was determined for the second major event using temporary station data. Moment tensor solutions derived from permanent station data (Herrmann, pers. comm.) indicate similar mechanisms and depths (6 km) for both earthquakes. The focal mechanism in Figure 1 was determined for the second event using both permanent and temporary data (McCue, pers. comm.).

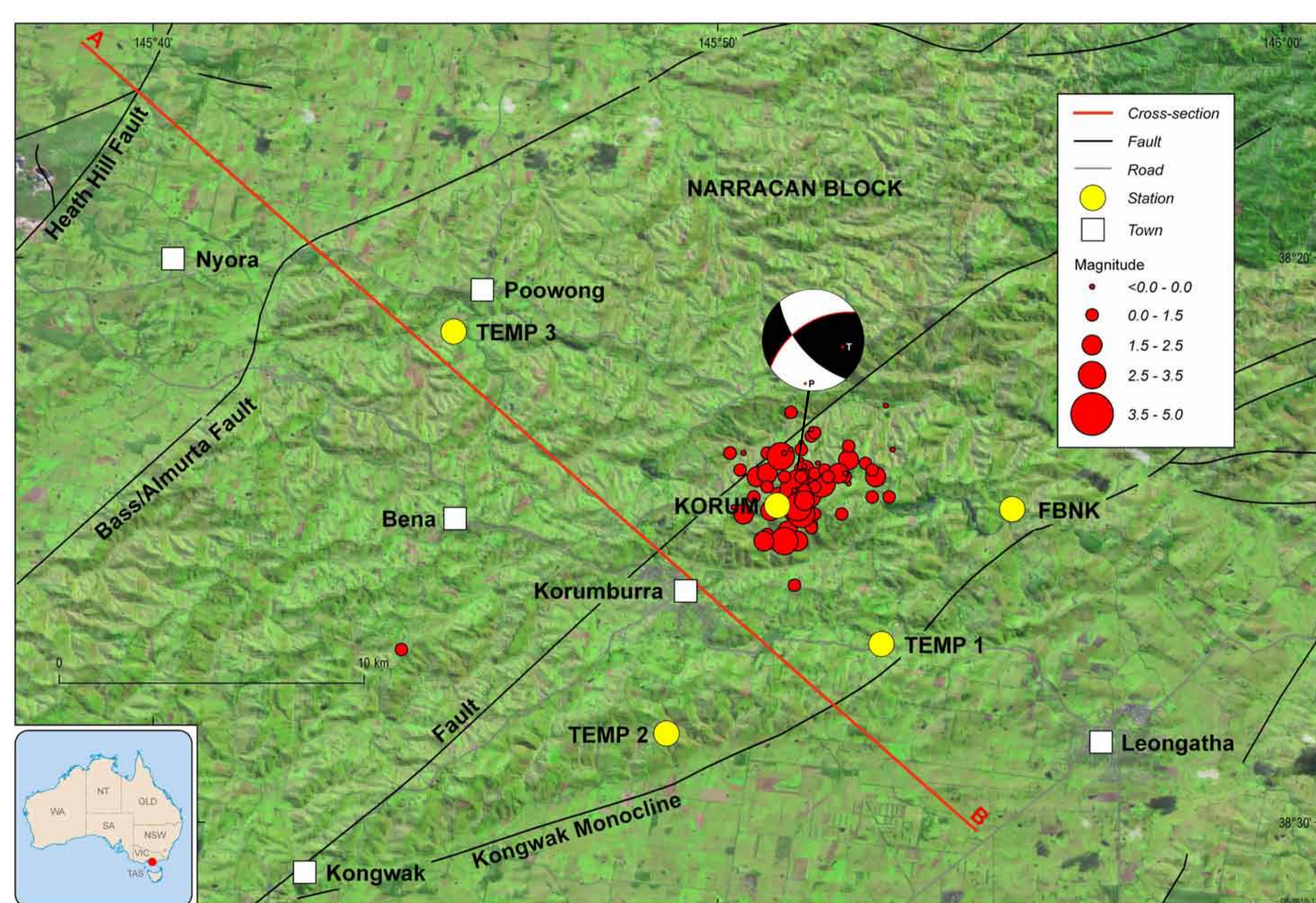


Figure 1. Plot of epicentres of the March 2009 Korumburra earthquakes, and temporary seismographs, overlaid onto the 3-second SRTM DEM data with major fault traces marked. Focal mechanism courtesy of Kevin McCue (preferred nodal plane marked). A-B marks the cross section shown in Figure 2.

Geological interpretation

The Korumburra sequence of events occurred at ~5-8 km depth below the Narracan Block, an uplifted block between the Bass-Almurta Fault and the Kongwak Monocline (Figure 1). Both faults are considered to be *neotectonic* as there is significant geologically recent topography associated with them (>100 m). The events could be placed on either fault on the basis of spatial association with the surface fault traces; the subsurface geometry of the faults is unknown.

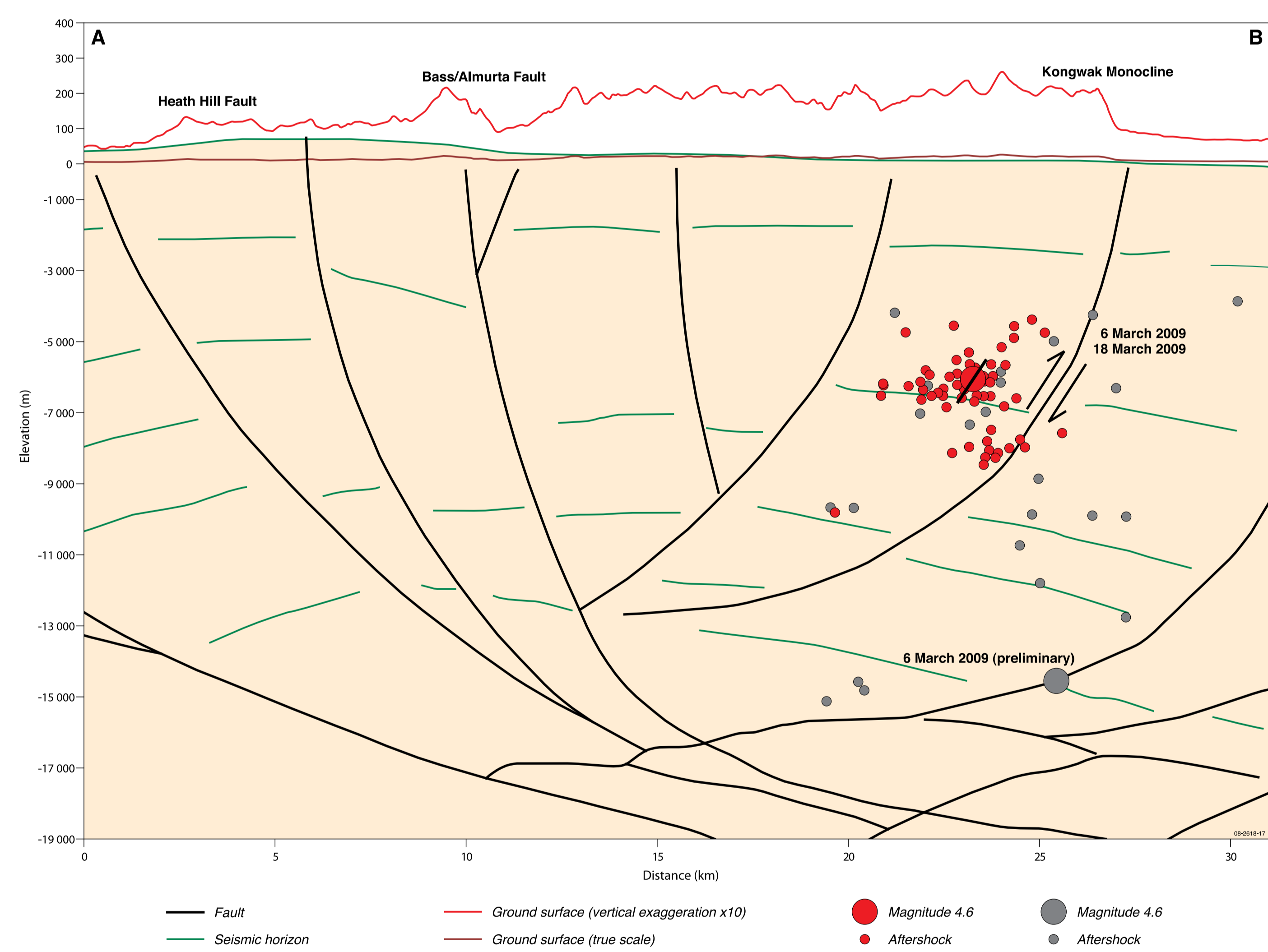


Figure 2. Cross section A-B showing hypocentral locations projected onto the section plane. Hypocentres determined before (grey) and after (red) the temporary deployment are shown. Rupture width of the magnitude 4.6 March 6 event is shown oriented with the preferred nodal plane of the focal mechanism. A line drawing of BMR seismic line 90/15 from the eastern Gippsland Basin (Williamson *et al.* 1991) is superimposed on the topography above the Korumburra earthquakes to approximate the subsurface fault geometry.

However, a plausible fault geometry is depicted in Figure 2, which superposes the structural geometry imaged by the seismic reflection line BMR Line 90/15 in the eastern Gippsland Basin (Williamson *et al.* 1991) onto the topography of the Narracan Block. One possible scenario could be developed whereby slip/creep on the Bass/Almurta Fault, in the ductile lower crust, stressed the hanging-wall block and triggered events on the fault underlying the Kongwak Monocline. However, the identity of the “active” faults associated with these earthquakes remains speculative pending more accurate estimates of hypocentral locations and subsurface fault geometry.

Preliminary Results of the M_s (VMAX) Magnitude for Local Earthquakes

The Korumburra earthquakes provided an opportunity to test an automated magnitude calculator employed by the Joint Australian Tsunami Warning Centre (JATWC). The M_s (VMAX) method (Russell 2006; Bonner *et al.* 2006) estimates variable-period surface-wave magnitudes by identifying the maximum amplitude in a period band of between 8 and 25 seconds. It has

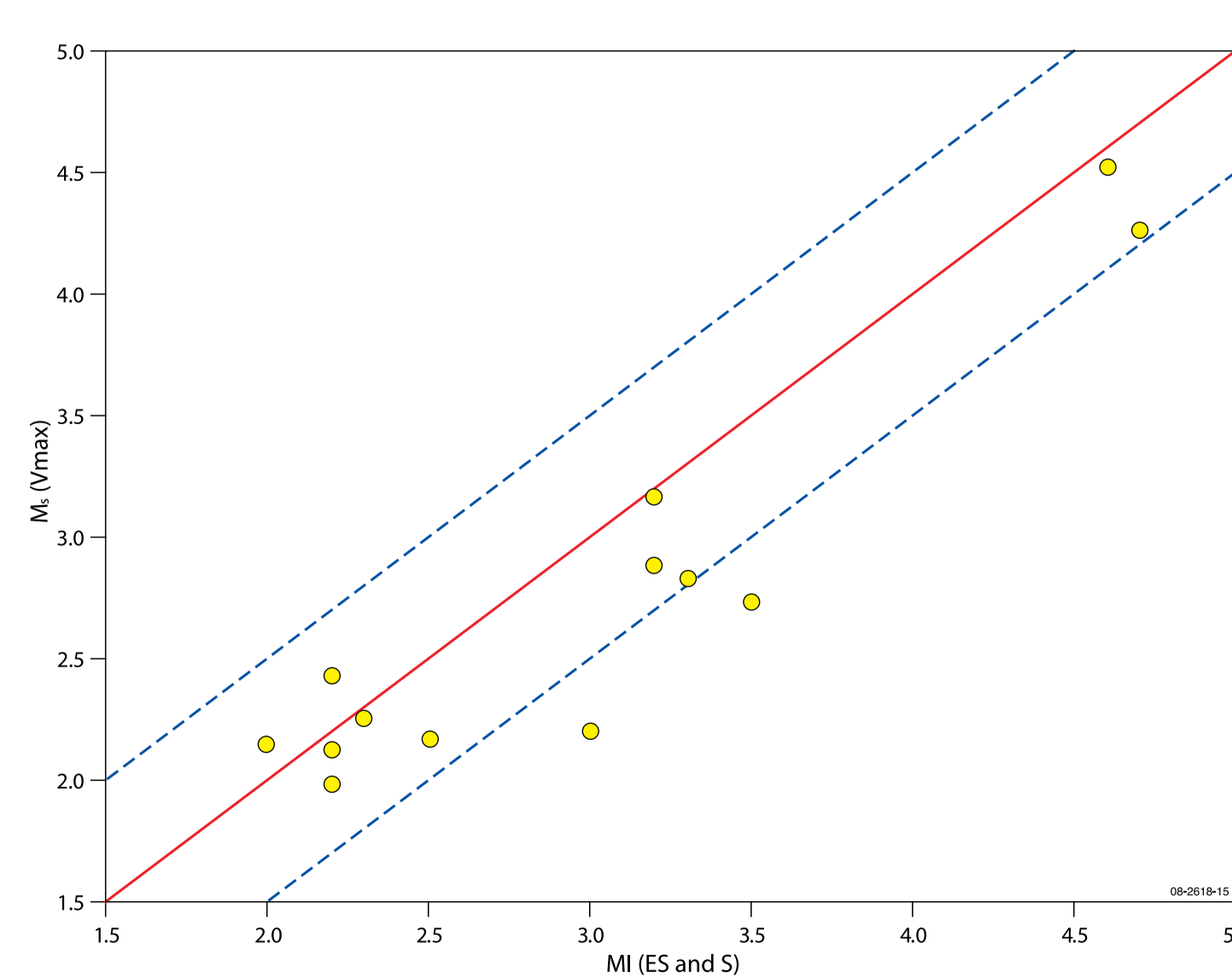


Figure 3. Comparison of the M_s (VMAX) network average magnitudes (GA permanent seismic stations only) versus the ES&S ML magnitudes.

been successfully used by the JATWC for regional and teleseismic events in combination with m_b and M_{wp} (Tsuboi *et al.* 1995), and is tested here for local earthquakes with epicentral distances from 1 to 10 degrees.

Preliminary results are presented in Figure 3 where the network (median) magnitude M_s (VMAX) is compared to ML calculated by ES&S. Smaller events, $2 \leq ML \leq 2.5$, provide a reasonable match to M_s (VMAX), however for $ML \geq 3$, M_s (VMAX) appears to consistently underestimate the magnitude. The main shocks on March 6 and 18 are underestimated by 0.1 and 0.4 respectively. However, the method generally appears to produce reasonable results when applied in a local scenario and shows promise for future use in an operational setting.

Ground Motion Data

The importance of aftershock deployments for capturing ground-motion data was demonstrated during the Korumburra earthquake sequence. Data recorded from the second ML 4.6 earthquake was analysed to investigate whether data from weak-motion velocity seismometers can be used to develop ground-motion acceleration prediction models. The station TEMP3 was configured with both a velocity seismometer and strong-motion accelerometer. Importantly, the seismometer did not clip under the strong ground-shaking.

The data recorded from the seismometer were converted to an acceleration time-history and superimposed on the acceleration time-history (Figure 4). In general, the match between the two records for each component is quite good. However, there is an obvious shift in phase, which is particularly apparent after the S-wave arrival.

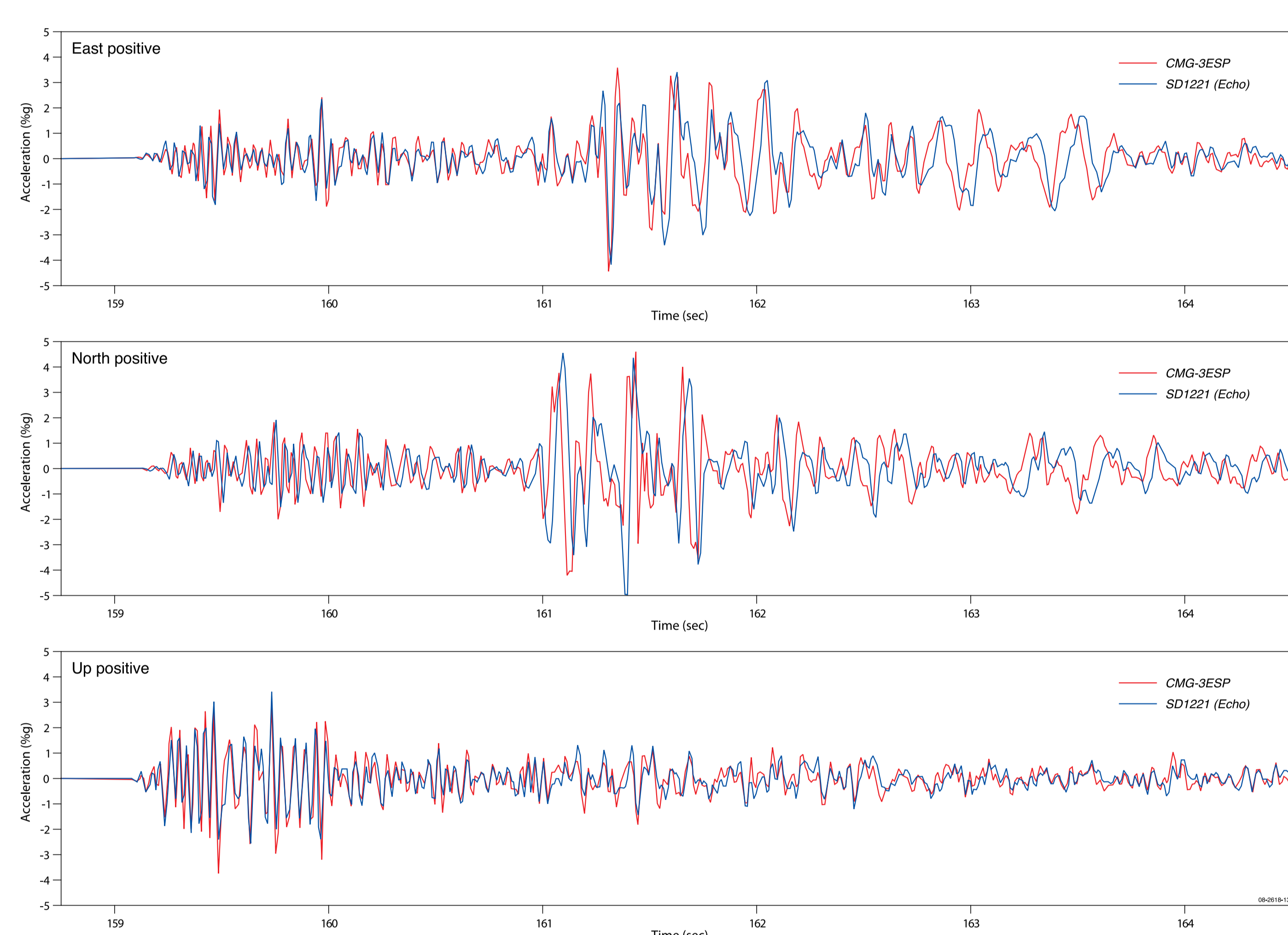


Figure 4. Data recorded on the velocity sensor (CMG-3ESP) converted to an acceleration time-history and superimposed on data from the acceleration sensor (SD1221).

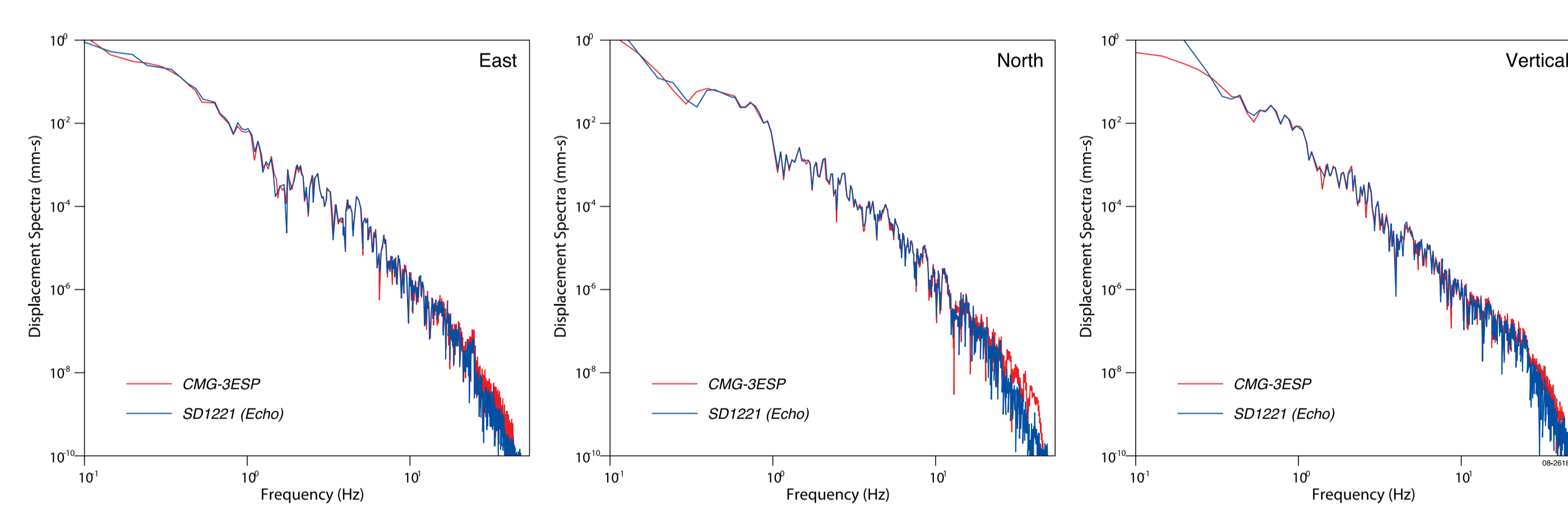


Figure 5. The Fourier spectra for each component of the velocity seismometer (CMG-3ESP) and accelerometer (SD1221).

The Fourier spectra for each component (Figure 5) suggest there is no significant difference in the waveforms recorded by either sensor, and suggests that weak-motion velocity data can be incorporated into strong-motion datasets for the development and validation of ground-motion prediction models. The reason for the higher spectral amplitudes observed from the velocity sensor at frequencies greater than about 25 Hz is not known, but it may be due to the use of “off the shelf” instrument response information.

Acknowledgements

We wish to thank David Pownall for assistance with the field work, Robert Dabrowski for his assistance with software, Kevin McCue who generated the focal mechanism, and Bob Herrmann who generated the moment tensor solutions (http://www.eas.slu.edu/Earthquake_Center/MECH.AU/).

Associations

1. Corresponding Author, Australian Tsunami Warning System, Geoscience Australia, jonathon.bathgate@ga.gov.au; also, hugh.glanville@ga.gov.au and steven.tatham@ga.gov.au
2. Earthquake Hazard Project, Geoscience Australia, trevor.allen@ga.gov.au, dan.clark@ga.gov.au and clive.collins@ga.gov.au
3. Seismology Research Centre, Environmental Systems & Services, Melbourne, and School of Geosciences, Monash University, Melbourne, gary@earthquake.net.au
4. Seismology Research Centre, Environmental Systems & Services, Melbourne, adam.pascale@esands.com, wayne.peck@esands.com and claire.quinn@esands.com

References

- Bonner, J.L., D.R. Russell, D.G. Harkrider, D.T. Reiter, and R.B. Herrmann (2006). Development of a time-domain, variable-period surface-wave magnitude measurement procedure for application at regional and teleseismic distances, part II: Application and M_s - m_b performance, *Bull. Seism. Soc. Am.*, 96, 678-696.
- Russell, D.R. (2006). Development of a time-domain, variable-period surface-wave magnitude measurement procedure for application at regional and teleseismic distances, part I: Theory, *Bull. Seism. Soc. Am.*, 96, 665-677.
- Tsuboi, S., K. Abe, K. Takano, and Y. Yamanaka (1995). Rapid determination of M_w from broadband P waveforms, *Bull. Seism. Soc. Am.*, 83, 606-613.
- Williamson P. E., Willcox J. B., Colwell J. B. & Collins C. D. N. 1991. The Gippsland Basin Deep Seismic Reflection/Refraction Grid. *Exploration Geophysics* 22, 497-502

For further information contact:
Jonathan Bathgate Ph: 02 6249 9690
Email: jonathan.bathgate@ga.gov.au
www.ga.gov.au